Scaling Laws for Regional Stratification at the top of Earth's Core

Jonathan E. Mound[1] and Christopher J. Davies[1]
1: School of Earth and Environment, University of Leeds, Leeds LS2 9JT, UK
Corresponding author email: J.E.Mound@leeds.ac.uk

Abstract

Seismic and geomagnetic observations have been used to argue both for and against a global stratified layer at the top of Earth's outer core. Recently, we used numerical models of turbulent thermal convection to show that imposed lateral variations in core-mantle boundary (CMB) heat flow can give rise to regional lenses of stratified fluid at the top of the core while the bulk of the core remains actively convecting. Here we develop theoretical scaling laws to extrapolate the properties of regional stratified lenses measured in simulations to the conditions of Earth's core. We estimate that regional stratified lenses in Earth's core have thicknesses of up to a few hundred kilometres and Brunt-Väisälä frequencies of hours, consistent with independent observational constraints. The location, thickness, and strength of the stratified regions would change over geological time scales in response to the slowly evolving CMB heat flux heterogeneity imposed by mantle convection.

1 Introduction

Independent inferences from seismology (*Tanaka*, 2007; *Helffrich and Kaneshima*, 2010; *Kaneshima*, 2018), geomagnetism (*Buffett*, 2014; *Buffett et al.*, 2016; *Olson et al.*, 2018; *Yan and Stanley*, 2018), and geodynamics (*Nimmo*, 2015; *Davies et al.*, 2015) have been used to suggest the existence of a stably stratified layer at the top of Earth's liquid core. However, some seismic studies (*Alexandrakis and Eaton*, 2010; *Irving et al.*, 2018) find that a stratified layer is not required. Additionally, concentrated patches of magnetic flux at the core-mantle boundary (CMB) (*Amit*, 2014) and secular variation of the total geomagnetic energy at the CMB (*Huguet et al.*, 2018) are hard to explain without radial motions near the top of the core that are difficult to reconcile with a thick and strongly stratified global layer. Nevertheless, a variety of origin mechanisms have been proposed that could produce thermal and/or compositional stratification (e.g. *Lister and Buffett*, 1998; *Buffett and Seagle*, 2010; *Pozzo et al.*, 2012; *Gubbins and Davies*, 2013; *Helffrich and Kaneshima*, 2013; *Landeau et al.*, 2016; *Brodholt and Badro*, 2017; *Bouffard et al.*, 2019).

Convection in the core is controlled by heat flow across the CMB. Compared to the dynamics of the relatively low-viscosity core, solid-state convection in the overlying mantle is associated with long time scales and large temperature variations, such that the core is subjected to large lateral variations in CMB heat flux (*Nakagawa and Tackley*, 2008; *Zhang and Zhong*, 2011; *Olson et al.*, 2015; *Stackhouse et al.*, 2015). This CMB heat flux heterogeneity would interact with, and potentially disrupt, any inherent core stratification (e.g. *Gibbons and Gubbins*, 2000; *Gubbins et al.*, 2015; *Olson et al.*, 2017; *Christensen*, 2018; *Cox et al.*, 2019) and can have a significant influence on the pattern of core convection and hence the geomagnetic field (e.g. *Glatzmaier et al.*, 1999; *Olson and Christensen*, 2002; *Gubbins and Gibbons*, 2004; *Gubbins et al.*, 2007; *Davies et al.*, 2008; *Olson et al.*, 2015).

An alternative view of core stratification has recently been suggested from numerical modelling in which stratification is caused, rather than opposed, by lateral CMB heat flow variations;

furthermore, the resultant stratification is found to be confined into regional lenses, rather than a global layer (*Mound et al.*, 2019). In some cases, 1D averaging over strong and laterally extensive regional inversion lenses can produce an apparent global stratification despite there being radial motion throughout the core including its outermost regions. Regional inversion lenses are ubiquitous in our simulations; however, estimation of their expected thickness L and Brunt-Väisälä frequency N in the Earth require extrapolation from the computationally accessible parameter regime to that characteristic of Earth's core.

Three nondimensional parameters control the dynamic behaviour in our numerical model of rotating nonmagnetic convection in a spherical shell (*Willis et al.*, 2007). The Prandtl number $Pr = \nu/\kappa$ is the ratio of the fluid's kinematic viscosity ν and its thermal diffusivity κ. The strength of convective driving is described by the Rayleigh number $\widetilde{Ra} = \alpha g_\mathrm{o} \beta / 2\Omega\kappa$, where α is the thermal expansivity of the fluid, g_o is the gravitational acceleration on the outer boundary ($r = r_\mathrm{o}$), Ω is the planetary rotation rate, and $\beta = r_\mathrm{o}^2 q_\mathrm{ave}/k$, where k is the thermal conductivity of the fluid and q_ave is the average heat flux across the outer boundary. The importance of the fluid viscosity relative to rotation is described by the Ekman number $E = \nu/2\Omega h^2$, where $h = r_\mathrm{o} - r_\mathrm{i}$ is the shell thickness. We describe the amplitude of heat flux heterogeneity at the CMB using $q^\star = (q_\mathrm{max} - q_\mathrm{min})/q_\mathrm{ave}$, where q_max and q_min are the maximum and minimum heat flux, respectively (with outward heat flux defined to be positive).

Our previous work considered two patterns of CMB heat flux heterogeneity, one derived from seismic tomography (*Masters et al.*, 1996) and a hemispheric pattern that could represent past mantle flow, with amplitudes given by $q^\star = 0.0$, 2.3 and 5.0 (for the hemispheric pattern the minimum CMB heat flux q_min is located at 0°N, 0°E). We produced a suite of non-magnetic rotating convection simulations covering $E = \{10^{-4}, 10^{-5}, 10^{-6}\}$, $\widetilde{Ra}$ up to several hundred times the critical value for the onset of convection, and $Pr = 1$.

Although our simulations approach the limit of what is computationally feasible, they remain far from the parameter regime for the Earth's core. In particular, estimates of the relevant parameters suggest that $\widetilde{Ra}$ may be far larger and E far smaller in the Earth than in our simulations (*Mound et al.*, 2019). The value of $q^\star$ is uncertain in the Earth as it requires knowledge of both the temperature structure and thermal conductivity of the lowermost mantle and the total superadiabatic CMB heat flow; nevertheless, its value in the Earth may be an order of magnitude larger than in our simulations (*Mound et al.*, 2019). In this work, we first establish the theory relating L and N to the underlying physical parameters of the convecting system. We then show that our simulations match this theoretical expectation, enabling us to extrapolate to parameter values plausibly representative of the Earth's core.

2 Scaling Theory

The dynamics of convection falls into qualitatively different regimes depending on what combination of forces are important and which play a subdominant or inconsequential role. Scaling laws relating emergent behaviours to the imposed control parameters differ between dynamic regimes; so, care must be taken when extrapolating simulation results to planetary conditions (e.g. *King et al.*, 2013; *Jones*, 2015; *Gastine et al.*, 2016; *Aubert et al.*, 2017). For the turbulent rotating convection of our simulations we expect Inertial, Archimedean buoyancy, and Coriolis forces to be important and focus on this regime (characterised by the IAC balance), which holds in 34 of our

previously presented simulations (*Mound and Davies*, 2017; *Long et al.*, 2019).

In a fluid where density decreases with increasing radius, a fluid parcel displaced radially with be returned to its original depth by buoyancy forces with a characteristic Brunt-Väisälä frequency given by

$$N^2 = -\frac{g}{\rho_0}\frac{\partial \rho}{\partial r}, \tag{1}$$

where ρ_0 is a reference density. For radial density variations arising from purely thermal effects

$$N^2 = \alpha g \frac{\partial T}{\partial r}. \tag{2}$$

For our Boussinesq models with fixed-flux thermal boundary conditions the strength of thermal stratification is approximately set by the temperature gradient associated with the value of $q_{\min}$ imposed at the CMB. We note that along some radial profiles the maximum temperature gradient occurs some distance below the outer boundary; nevertheless, we will use $\partial T/\partial r \approx -q_{\min}/k$ to estimate the maximum value of N expected in our simulations. For a simple pattern of CMB heat flux variation and our definition of $q^\star$ we expect

$$q_{\text{ave}} \approx \frac{1}{2}(q_{\max} + q_{\min}) \tag{3}$$

and hence

$$q_{\min} \approx -q_{\text{ave}}(q^\star - 2)/2. \tag{4}$$

Using 2Ω as our frequency scaling leads to

$$\left(\frac{N}{2\Omega}\right) \approx \left[\frac{\alpha g_{\text{o}} \beta}{4\Omega^2 r_{\text{o}}^2}\left(\frac{q^\star - 2}{2}\right)\right]^{1/2}. \tag{5}$$

For the Earth, it will be the average superadiabatic heat flux q^+_{ave} that controls the vigour of convection; so, it is useful to recast our expression for N as

$$\left(\frac{N}{2\Omega}\right) \approx \left[\frac{\alpha g_{\text{o}}}{8\Omega^2 k}(q_{\text{ptp}} - 2q^+_{\text{ave}})\right]^{1/2}, \tag{6}$$

where $q_{\text{ptp}} = q_{\max} - q_{\min}$ is the peak-to-peak variation in CMB heat flux. For comparison to our simulations, it is useful to combine the physical parameters into the relevant control parameters giving an expected scaling of

$$\left(\frac{N}{2\Omega}\right) \sim \left[\frac{\widetilde{Ra}E}{Pr}\left(\frac{q^\star - 2}{2}\right)\right]^{1/2}. \tag{7}$$

Only for sufficiently strong heat flux heterogeneity will there be regions of the CMB beneath which convection is entirely suppressed. In the Earth, this requires regions of sufficiently hot lowermost mantle such that the imposed temperature gradient is subadiabatic. This requirement enters the equations above via the need for $q^\star > 2$ or, equivalently, $q_{\text{ptp}} > 2q^+_{\text{ave}}$ in order to ensure N is a positive real number.

The thickness of the stratified regions may be set by a competition between the heat transport condition imposed by the mantle at the CMB and the advection of heat by the convecting bulk of the core. Within the thermally stratified regional inversion lenses radial convection is suppressed and heat transport is dominated by conduction ($\kappa\nabla^2 T$). Where convection dominates, the radial transport of heat will primarily arise via advection ($\mathbf{u}\cdot\nabla T$). Assuming an approximate balance between these terms gives an expected scaling of

$$\frac{UT'}{\ell} \sim \frac{\kappa\Delta T'}{L^2}, \tag{8}$$

where U is the characteristic velocity of convection, ℓ is the characteristic length scale of convection, T' is the characteristic convective temperature fluctuation, $\Delta T'$ is the total temperature anomaly across the thickness of the lens, and L is the characteristic lens thickness. Multiplying each side by $1/h^2$ and rearranging gives

$$\frac{L^2}{h^2} \sim \frac{\ell}{h}\frac{\kappa\Delta T'/h}{UT'}. \tag{9}$$

The average advective heat flux in the interior of our models will be determined by the average imposed heat flux at the CMB; so, we expect $UT' \sim q_{\mathrm{ave}}$. As noted in the discussion of the scaling for the Brunt-Väisälä frequency, the strongest inverted temperature gradient (and hence conductive heat transport) can be associated with the minimum imposed CMB heat flux such that $\kappa\Delta T' \sim q_{\mathrm{min}}$. Making use of these associations and equations 3 and 4 we can rewrite equation 9 as

$$\frac{L^2}{h^2} \sim \frac{\ell}{h}\left[\frac{q^\star - 2}{2}\right]. \tag{10}$$

The expected scaling of ℓ will depend on which force balance describes the convective dynamics. For our simulations that sit within the IAC regime, the convective length scale is expected (*Aubert et al.*, 2001) to scale as

$$\frac{\ell}{h} \sim E^{3/5} Pr^{-2/5} Ra_{\mathrm{F}}^{1/5}, \tag{11}$$

where the flux Rayleigh number $Ra_{\mathrm{F}} = \widetilde{Ra}/E$ (*Mound and Davies*, 2017). Therefore, we expect that the thickness of the regional inversion lenses should scale as

$$\frac{L}{h} \sim E^{1/5} Pr^{-1/5} \widetilde{Ra}^{1/10} \left[\frac{q^\star - 2}{2}\right]^{1/2}. \tag{12}$$

In terms of the underlying physical parameters this scaling becomes

$$\frac{L}{h} \sim \left[\frac{\alpha g_{\mathrm{o}} r_{\mathrm{o}}^2}{256\rho C_P \Omega^3 h^4}\right]^{1/10} \left[q_{\mathrm{ave}}^+\right]^{-2/5} \left[q_{\mathrm{ptp}} - 2q_{\mathrm{ave}}^+\right]^{1/2}. \tag{13}$$

The scaling laws for N and L depend on a number of physical parameters, values of which are listed in Table 1. To compare our Boussinesq model with the Earth it is the superadiabatic heat flow across the CMB that should be used to determine the relevant thermal forcing $\beta = Q^+/4\pi k$, a quantity that is poorly constrained with even the sign of Q^+ uncertain (*Olson*, 2015; *Jones*, 2015). Regional inversion lenses will occur only if the combination of Q^+ and q_{ptp} result in a CMB

Table 1: Physical Parameters for the Earth

Quantity	Symbol	Value
Density of core fluid[a]	ρ	1.003×10^4 kg m$^{-}3$
Gravitational acceleration[a]	g_{o}	10.68 m s^2
Radius of CMB[a]	r_{o}	3.480×10^6 m
Radius of ICB[a]	r_{i}	1.222×10^6 m
Rotation rate[b]	Ω	7.292×10^{-5} s^{-1}
Specific heat[c]	C_P	715 J kg^{-1} K^{-1}
Thermal expansivity[c]	α	1.8×10^{-5} K^{-1}
Thermal conductivity[d]	k	110 W m^{-1} K^{-1}

[a](*Dziewonski and Anderson*, 1981), [b](*Aoki et al.*, 1982)
[c](*Gubbins et al.*, 2003), [d](*Pozzo et al.*, 2012)

heat flux pattern that has both super- and subadiabatic regions. Based on a scaling argument for core velocity *Jones* (2011) estimated $Q^+ \approx 0.6$ TW; whereas a comparison of core adiabatic heat flow estimates (*Davies et al.*, 2015) and total CMB heat flow estimates (*Nimmo*, 2015) suggest values as large as $Q^+ \approx 3$ TW are possible. We will use both of these estimates to bound our extrapolations. Similarly, the lateral variation in heat flux, q_{ptp} should be considered relative to the average superadiabatic flux, $q^+_{\mathrm{ave}} = Q^+/4\pi r_{\mathrm{o}}^2$ when determining $q^\star$; here we adopt $q_{\mathrm{ptp}} = 0.14$ W/m^2 (*Stackhouse et al.*, 2015) leading to $q^\star \approx 10$ or 35 for our chosen values of Q^+.

3 Scaling Results

We have determined the thickness and maximum Brunt-Väisälä frequency for the regional inversion lenses in our simulations at two locations beneath the CMB; which we will refer to as African (0°N, 0°E) and Pacific (0°N, 180°E). We first establish that our simulations obey the expected scaling by restricting ourselves to the subset of simulations with a hemispheric pattern of CMB heat flux heterogeneity. For this set of simulations, q_{min} is located where we measure L and N for the African regional inversion lens and the pattern of heat flux heterogeneity obeys the adopted geometric assumptions (equations 3 and 4). Therefore, we expect this subset of lenses should best conform to the derived scalings; as can be seen in figure 1 the agreement is indeed excellent.

For the tomographic pattern of CMB heterogeneity q_{min} is located beneath the south Pacific; however, a regional inversion layer may still form beneath Africa provided q_{ptp} is sufficiently large. Therefore, we have chosen to measure N and L at fix geographic locations in all simulations, rather than only beneath the location of q_{min}. As a result, when considering all simulation results together (figure 2) the developed scaling laws do not fit the measurements of N and L as well as they do when considering only the hemispheric pattern. Nevertheless, each combination of CMB heat flux pattern and lens location does follow the expected scaling and the best-fit prefactors for each lens location do a reasonable job of explaining L and N across all of our simulations falling in the IAC regime. The scalings fit to all simulations allow us to extrapolate to the conditions relevant to the Earth's core for our two choices of Q^+. For the lower value of superadiabatic CMB heat flow (grey stars in figure 2) the extrapolated L and N are somewhat larger than for the higher $Q+$ (grey squares).

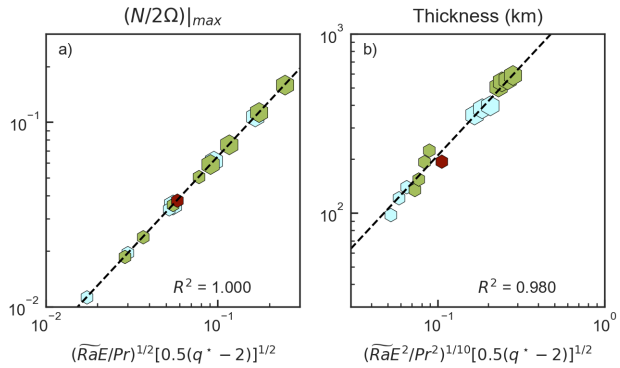

Figure 1: Scaling of the (a) Brunt-Väisälä frequency and (b) thickness of the African regional inversion lens for simulations with a hemispheric pattern of CMB heat flux heterogeneity. The dashed lines and R^2 values are based on the best fit prefactors. Symbol colour indicates $E = \{10^{-6}, 10^{-5}, 10^{-4}\}$ (light blue, olive, brick), and size indicates $q^\star = \{2.3, 5\}$ (small, large).

Table 2: Extrapolations to Earth

	Thickness (km)		Brunt-Väisälä $(N/2\Omega)$	
	Tomographic Q^+_{Low} , Q^+_{High}	Hemispheric Q^+_{Low} , Q^+_{High}	Tomographic Q^+_{Low} , Q^+_{High}	Hemispheric Q^+_{Low} , Q^+_{High}
Pacific	418 , 192	0 , 0	3.05 , 2.66	N/A , N/A
Africa	230 , 105	358 , 164	1.37 , 1.20	2.33 , 2.04

We also sub-divide the simulations and use the best-fit prefactor for each combination of geographic location and pattern of CMB heterogeneity to predict lens properties in the Earth for $Q^+_{\text{Low}} = 0.6$ TW and $Q^+_{\text{High}} = 3$ TW (table 2). For the chosen tomographic boundary condition the heat flux low under the Pacific is deeper than the low under Africa. As a result, the predicted thickness and Brunt-Väisälä frequency of the Pacific lens are always larger than the African lens. For our chosen orientation of hemispheric forcing, there is no Pacific lens.

4 Discussion

The developed theoretical scalings do a good job of fitting our simulations of regional inversion layers and allow us to extrapolate to Earth's core conditions, predicting values of L and N that are geophysically plausible. Observational constraints on L and N for a global stratification at the top of the core have been derived from both seismic and geomagnetic observations. Seismic evidence allows a layer of anomalously slow P-wave speed up to 450 km thick (*Kaneshima*, 2018); when combined with a model for chemical enrichment (*Helffrich and Kaneshima*, 2010), the Brunt-Väisälä frequency is inferred to be $N/2\Omega \approx 3.5 - 7.35$. Magnetic-Archimedean-Coriolis (MAC) waves in a stable layer 130-140 km thick with $N/2\Omega \approx 0.37 - 0.42$ have been suggested to explain certain periodic variations of the magnetic field (*Buffett et al.*, 2016). The fundamental difference in our scenario is that stratification should be present only under regions of anomalously low CMB heat flux and absent where the CMB heat flux is superadiabatic.

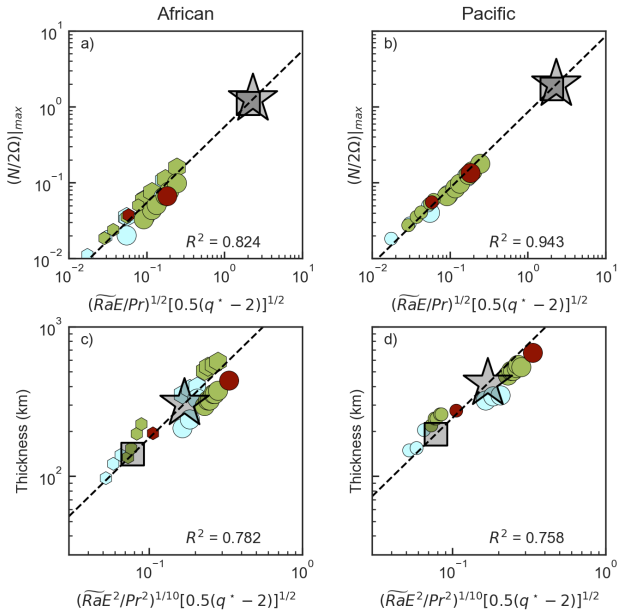

Figure 2: Scaling of the African (a, c) and Pacific (b, d) regional inversion lenses in all of the simulations. Maximum Brunt-Väisälä frequency (a, b) and thickness (c,d) from the simulations (coloured symbols) plotted against the theoretical scaling. The dashed lines and R^2 values are based on the best fit prefactors for each region, which are used to extrapolate to the Earth for $Q^+_{\mathrm{low}} = 0.6$ TW (star) or $Q^+_{\mathrm{high}} = 3$ TW (square). Colours of the filled symbols indicate $E = \{10^{-6}, 10^{-5}, 10^{-4}\}$ (light blue, olive, brick), size indicates $q^\star = \{2.3, 5\}$ (small, large), and shape indicates tomographic (circles) or hemispheric (hexagons) patterns of CMB heat flux heterogeneity.

The smaller the total superadiabatic heat flow across the CMB the broader, stronger and thicker the regional inversion layers are expected to be. Ascertaining the existence and extent of regional inversion layers at the top of the core would, therefore, provide constraints on the values of Q^+ and q_{ptp} and hence the thermal state of the lowermost mantle. As the pattern and strength of CMB heat flux heterogeneity evolves over geological time in response to ongoing mantle convection, the predicted locations, thicknesses, and strengths of regional inversion layers would similarly evolve in response.

Extrapolation of regional inversion lens thickness to the Earth requires understanding of the appropriate force balance, both for the Earth and the given suite of simulations. For a given convecting system the dominant force balance will depend on its physical properties and boundary conditions, and can differ between boundary layers and the interior, and with the length-scale considered (e.g. *Grossmann and Lohse*, 2000; *Gastine et al.*, 2016; *Aurnou and King*, 2017; *Schwaiger et al.*, 2019; *Aubert*, 2019). The goodness of our fits (figures 1 and 2) and previous analysis (*Mound and Davies*, 2017; *Long et al.*, 2019) indicate that the IAC balance holds in the simulations we have considered here. The dynamic balance enters into the scaling for L (equation 10) by determining the small length-scale associated with convection. Therefore, it is straightforward to consider another force balance, such as one incorporating the influence of the magnetic field on the dynamics within the Earth's core. For example, *Davidson* (2013) derived a scaling for ℓ assuming a MAC

balance holds; substitution of his equation (12) into our equation 10 results in

$$\frac{L}{h} \sim E^{1/9} Pr^{-1/9} \widetilde{Ra}^{1/18} \left[\frac{q^\star - 2}{2} \right]^{1/2} . \tag{14}$$

As with the scaling based on the IAC balance, this scaling depends only weakly on E, Pr, and $\widetilde{Ra}$ and hence the associated physical parameters. Since the details of the interior force balance play only a minor role in the scaling, we expect that regional inversion layers should be present and thick (approximately several hundred kilometres) in the Earth, provided $q^\star \gtrsim 3$.

5 Acknowledgments

CJD is supported by a Natural Environment Research Council Independent Research Fellowship (NE/L011328/1). This work used the ARCHER UK National Supercomputing Service (http://www.archer.ac.uk) and ARC, part of the High Performance Computing facilities at the University of Leeds, UK. Figures were produced using VisIt (*Childs et al.*, 2012), Matplotlib (*Hunter*, 2007) and seaborn (*Waskom et al.*, 2018).

References

Alexandrakis, C., and D. W. Eaton, Precise seismic-wave velocity atop Earth's core: No evidence for outer-core stratification, *Physics of the Earth and Planetary Interiors*, *180*(1-2), 59–65, doi: 10.1016/j.pepi.2010.02.011, 2010.

Amit, H., Can downwelling at the top of the Earth's core be detected in the geomagnetic secular variation?, *Physics of the Earth and Planetary Interiors*, *229*(C), 110–121, doi: 10.1016/j.pepi.2014.01.012, 2014.

Aoki, S., B. Guinot, G. H. Kaplan, H. Kinoshita, D. D. McCarthy, and P. K. Seidelmann, The new definition of universal time, *Astronomy and Astrophysics*, *105*, 359–361, 1982.

Aubert, J., Approaching Earth's core conditions in high-resolution geodynamo simulations, *Geophysical Journal International*, *219*(Supplement-1), S137–S151, doi:10.1093/gji/ggz232, 2019.

Aubert, J., D. Brito, H.-C. Nataf, P. Cardin, and J.-P. Masson, A systematic experimental study of rapidly rotating spherical convection in water and liquid gallium, *Physics of the Earth and Planetary Interiors*, *128*(1-4), 51–74, doi:10.1016/S0031-9201(01)00277-1, 2001.

Aubert, J., T. Gastine, and A. Fournier, Spherical convective dynamos in the rapidly rotating asymptotic regime, *Journal of Fluid Mechanics*, *813*, 558–593, doi:10.1017/jfm.2016.789, 2017.

Aurnou, J. M., and E. M. King, The cross-over to magnetostrophic convection in planetary dynamo systems, *Proceedings of the Royal Society A: Mathematical, Physical and Engineering Science*, *473*(2199), 20160,731, doi:10.1098/rspa.2016.0731, 2017.

Bouffard, M., G. Choblet, S. Labrosse, and J. Wicht, Chemical Convection and Stratification in the Earth's Outer Core, *Frontiers in Earth Science*, *7*, 1–19, doi:10.3389/feart.2019.00099, 2019.

Brodholt, J., and J. Badro, Composition of the low seismic velocity E´ layer at the top of Earth's core, *Geophysical Research Letters*, *44*(16), 8303–8310, doi:10.1002/2017GL074261, 2017.

Buffett, B., Geomagnetic fluctuations reveal stable stratification at the top of the Earth's core, *Nature*, *507*(7493), 484–487, doi:10.1038/nature13122, 2014.

Buffett, B., N. Knezek, and R. Holme, Evidence for MAC waves at the top of Earth's core and implications for variations in length of day, *Geophysical Journal International*, *204*(3), 1789–1800, doi:10.1093/gji/ggv552, 2016.

Buffett, B. A., and C. T. Seagle, Stratification of the top of the core due to chemical interactions with the mantle, *Journal of Geophysical Research*, *115*(B4), B04,407, doi:10.1029/2009JB006751, 2010.

Childs, H., E. Brugger, B. Whitlock, J. Meredith, S. Ahern, D. Pugmire, K. Biagas, M. Miller, C. Harrison, G. H. Weber, H. Krishnan, T. Fogal, A. Sanderson, C. Garth, E. W. Bethel, D. Camp, R. Oliver, M. Durant, J. M. Favre, and P. Navrátil, VisIt: An end-user tool for visualizing and analyzing very large data, in *High Performance Visualization*, edited by E. W. Bethel, H. Childs, and C. Hansen, pp. 357–372, Chapman and Hall, doi:10.1201/b12985-21, 2012.

Christensen, U. R., Geodynamo models with a stable layer and heterogeneous heat flow at the top of the core, *Geophysical Journal International*, *215*(2), 1338–1351, doi:10.1093/gji/ggy352, 2018.

Cox, G. A., C. J. Davies, P. W. Livermore, and J. Singleton, Penetration of boundary-driven flows into a rotating spherical thermally stratified fluid, *Journal of Fluid Mechanics*, *864*, 519–553, doi:10.1017/jfm.2018.999, 2019.

Davidson, P. A., Scaling laws for planetary dynamos, *Geophysical Journal International*, *195*(1), 67–74, doi:10.1093/gji/ggt167, 2013.

Davies, C., M. Pozzo, D. Gubbins, and D. Alfè, Constraints from material properties on the dynamics and evolution of Earth's core, *Nature Geoscience*, *8*(9), 678–685, doi:10.1038/ngeo2492, 2015.

Davies, C. J., D. Gubbins, A. P. Willis, and P. K. Jimack, Time-averaged paleomagnetic field and secular variation: Predictions from dynamo solutions based on lower mantle seismic tomography, *Physics of the Earth and Planetary Interiors*, *169*(1-4), 194–203, doi:10.1016/j.pepi.2008.07.021, 2008.

Dziewonski, A. M., and D. L. Anderson, Preliminary reference Earth model, *Physics of the Earth and Planetary Interiors*, *25*(4), 297–356, 1981.

Gastine, T., J. Wicht, and J. Aubert, Scaling regimes in spherical shell rotating convection, *Journal of Fluid Mechanics*, *808*, 690–732, doi:10.1017/jfm.2016.659, 2016.

Gibbons, S. J., and D. Gubbins, Convection in the Earth's core driven by lateral variations in the core–mantle boundary heat flux, *Geophysical Journal International*, *142*(2), 631–642, 2000.

Glatzmaier, G. A., R. S. Coe, L. Hongre, and P. H. Roberts, The role of the Earth's mantle in controlling the frequency of geomagnetic reversals, *Nature*, *401*(6756), 885–890, 1999.

Grossmann, S., and D. Lohse, Scaling in thermal convection: a unifying theory, *Journal of Fluid Mechanics*, *407*, 27–56, doi:10.1017/S0022112099007545, 2000.

Gubbins, D., and C. J. Davies, The stratified layer at the core-mantle boundary caused by barodiffusion of oxygen, sulphur and silicon, *Physics of the Earth and Planetary Interiors*, *215*(C), 21–28, doi:10.1016/j.pepi.2012.11.001, 2013.

Gubbins, D., and S. J. Gibbons, Low Pacific Secular Variation, in *Timescales Of The Paleomagnetic Field*, edited by J. E. T. Channell, D. V. Kent, W. Lowrie, and J. G. Meert, pp. 279–286, American Geophysical Union, Washington, D. C., doi:10.1029/145GM21, 2004.

Gubbins, D., D. Alfè, G. Masters, G. D. Price, and M. J. Gillan, Can the Earth's dynamo run on heat alone?, *Geophysical Journal International*, *155*(2), 609–622, 2003.

Gubbins, D., A. P. Willis, and B. Sreenivasan, Correlation of Earth's magnetic field with lower mantle thermal and seismic structure, *Physics of the Earth and Planetary Interiors*, *162*(3-4), 256–260, doi:10.1016/j.pepi.2007.04.014, 2007.

Gubbins, D., D. Alfè, C. Davies, and M. Pozzo, On core convection and the geodynamo: Effects of high electrical and thermal conductivity, *Physics of the Earth and Planetary Interiors*, *247*, 56–64, doi:10.1016/j.pepi.2015.04.002, 2015.

Helffrich, G., and S. Kaneshima, Outer-core compositional stratification from observed core wave speed profiles, *Nature*, *468*(7325), 807–810, doi:10.1038/nature09636, 2010.

Helffrich, G., and S. Kaneshima, Causes and consequences of outer core stratification, *Physics of the Earth and Planetary Interiors*, *223*(C), 2–7, doi:10.1016/j.pepi.2013.07.005, 2013.

Huguet, L., H. Amit, and T. Alboussière, Geomagnetic Dipole Changes and Upwelling/Downwelling at the Top of the Earth's Core, *Frontiers in Earth Science*, *6*, 1–14, doi:10.3389/feart.2018.00170, 2018.

Hunter, J. D., Matplotlib: A 2D graphics environment, *Computing in Science and Engineering*, *9*(3), 90–95, doi:10.1109/MCSE.2007.55, 2007.

Irving, J. C. E., S. Cottaar, and V. Lekić, Seismically determined elastic parameters for Earth's outer core, *Science Advances*, *4*, 1–9, 2018.

Jones, C. A., Planetary magnetic fields and fluid dynamos, *Annual Review of Fluid Mechanics*, *43*(1), 583–614, doi:10.1146/annurev-fluid-122109-160727, 2011.

Jones, C. A., Thermal and Compositional Convection in the Outer Core, in *Core Dynamics*, edited by P. Olson, pp. 115–159, Elsevier, Amsterdam, doi:10.1016/B978-0-444-53802-4.00141-X, 2015.

Kaneshima, S., Array analyses of SmKS waves and the stratification of Earth's outermost core, *Physics of the Earth and Planetary Interiors*, *276*, 234–246, doi:10.1016/j.pepi.2017.03.006, 2018.

King, E. M., S. Stellmach, and B. Buffett, Scaling behaviour in Rayleigh–Bénard convection with and without rotation, *Journal of Fluid Mechanics*, *717*, 449–471, doi:10.1017/jfm.2012.586, 2013.

Landeau, M., P. Olson, R. Deguen, and B. H. Hirsh, Core merging and stratification following giant impact, *Nature Geoscience*, *9*(10), 786–789, doi:10.1038/ngeo2808, 2016.

Lister, J. R., and B. A. Buffett, Stratification of the outer core at the core-mantle boundary, *Physics of the Earth and Planetary Interiors*, *105*(1-2), 5–19, doi:10.1016/S0031-9201(97)00082-4, 1998.

Long, R. S., J. E. Mound, C. J. Davies, and S. M. Tobias, Scaling behaviour in spherical shell rotating convection with fixed-flux thermal boundary conditions, *Journal of Fluid Mechanics*, *submitted*, 1–37, 2019.

Masters, G., S. Johnson, G. Laske, and H. Bolton, A shear-velocity model of the mantle, *Philosophical Transactions of the Royal Society A: Mathematical, Physical and Engineering Sciences*, *354*(1711), 1385–1411, doi:10.1098/rsta.1996.0054, 1996.

Mound, J., C. Davies, S. Rost, and J. Aurnou, Regional stratification at the top of Earth's core due to core–mantle boundary heat flux variations, *Nature Geoscience*, *12*(7), 575–580, doi:10.1038/s41561-019-0381-z, 2019.

Mound, J. E., and C. J. Davies, Heat transfer in rapidly rotating convection with heterogeneous thermal boundary conditions, *Journal of Fluid Mechanics*, *828*, 601–629, doi:10.1017/jfm.2017.539, 2017.

Nakagawa, T., and P. J. Tackley, Lateral variations in CMB heat flux and deep mantle seismic velocity caused by a thermal–chemical-phase boundary layer in 3D spherical convection, *Earth and Planetary Science Letters*, *271*(1-4), 348–358, doi:10.1016/j.epsl.2008.04.013, 2008.

Nimmo, F., Energetics of the Core, in *Core Dynamics*, edited by P. Olson, pp. 27–55, Elsevier, Amsterdam, doi:10.1016/B978-0-444-53802-4.00139-1, 2015.

Olson, P., Core Dynamics: An Introduction and Overview, in *Core Dynamics*, pp. 1–25, Elsevier B.V., doi:10.1016/B978-0-444-53802-4.00137-8, 2015.

Olson, P., and U. R. Christensen, The time-averaged magnetic field in numerical dynamos with non-uniform boundary heat flow, *Geophysical Journal International*, *151*(3), 809–823, 2002.

Olson, P., R. Deguen, M. L. Rudolph, and S. Zhong, Core evolution driven by mantle global circulation, *Physics of the Earth and Planetary Interiors*, *243*(C), 44–55, doi:10.1016/j.pepi.2015.03.002, 2015.

Olson, P., M. Landeau, and E. Reynolds, Dynamo tests for stratification below the core-mantle boundary, *Physics of the Earth and Planetary Interiors*, *271*, 1–18, doi: 10.1016/j.pepi.2017.07.003, 2017.

Olson, P., M. Landeau, and E. Reynolds, Outer Core Stratification From the High Latitude Structure of the Geomagnetic Field, *Frontiers in Earth Science*, *6*(140), 1–13, doi: 10.3389/feart.2018.00140, 2018.

Pozzo, M., C. Davies, D. Gubbins, and D. Alfè, Thermal and electrical conductivity of iron at Earth's core conditions, *Nature*, *485*(7398), 355–358, doi:10.1038/nature11031, 2012.

Schwaiger, T., T. Gastine, and J. Aubert, Force balance in numerical geodynamo simulations: a systematic study, *Geophysical Journal International*, *219*(Supplement-1), S101–S114, doi: 10.1093/gji/ggz192, 2019.

Stackhouse, S., L. Stixrude, and B. B. Karki, First-principles calculations of the lattice thermal conductivity of the lower mantle, *Earth and Planetary Science Letters*, *427*(C), 11–17, doi: 10.1016/j.epsl.2015.06.050, 2015.

Tanaka, S., Possibility of a low P-wave velocity layer in the outermost core from global SmKS waveforms, *Earth and Planetary Science Letters*, *259*(3-4), 486–499, doi: 10.1016/j.epsl.2007.05.007, 2007.

Waskom, M., O. Botvinnik, D. O'Kane, P. Hobson, J. Ostblom, S. Lukauskas, D. C. Gemperline, T. Augspurger, Y. Halchenko, J. B. Cole, J. Warmenhoven, J. de Ruiter, C. Pye, S. Hoyer, J. Vanderplas, S. Villalba, G. Kunter, E. Quintero, P. Barchant, M. Martin, K. Meyer, A. Miles, Y. Ram, T. Brunner, T. Yarkoni, M. L. Williams, C. Evans, C. Fitzgerald, Brian, and A. Qalieh, mwaskom/seaborn: v0.9.0, p. 1, doi:10.5281/zenodo.1313201, 2018.

Willis, A. P., B. Sreenivasan, and D. Gubbins, Thermal core–mantle interaction: Exploring regimes for 'locked' dynamo action, *Physics of the Earth and Planetary Interiors*, *165*(1-2), 83–92, doi: 10.1016/j.pepi.2007.08.002, 2007.

Yan, C., and S. Stanley, Sensitivity of the Geomagnetic Octupole to a Stably Stratified Layer in the Earth's Core, *Geophysical Research Letters*, *405*, 63–7, doi:10.1029/2018GL078975, 2018.

Zhang, N., and S. Zhong, Heat fluxes at the Earth's surface and core–mantle boundary since Pangea formation and their implications for the geomagnetic superchrons, *Earth and Planetary Science Letters*, *306*(3-4), 205–216, doi:10.1016/j.epsl.2011.04.001, 2011.